

ON THE STREAM-ACCRETION DISK INTERACTION: RESPONSE TO INCREASED MASS TRANSFER RATE

RUTH DGANI AND MARIO LIVIO
 Department of Physics, Technion, Haifa

AND

NOAM SOKER
 Department of Astronomy, University of Virginia
 Received 1988 February 16; accepted 1988 May 26

ABSTRACT

We calculate the time-dependent interaction between the stream of mass from the inner Lagrangian point and the accretion disk, resulting from an increasing mass transfer rate. The calculation is fully three-dimensional, using a pseudo-particle description of the hydrodynamics.

We demonstrate that the results of such calculations, when combined with specific observations, have the potential of both determining essential parameters, such as the viscosity parameter α , and can distinguish between different models of dwarf nova eruptions.

Subject headings: hydrodynamics — stars: accretion — stars: dwarf novae

I. INTRODUCTION

Cataclysmic variables (CV) and low-mass X-ray binaries (LMXB) are binary systems in which a low-mass companion transfers mass onto a compact object, via Roche lobe overflow. In such systems, the stream of mass from the inner Lagrangian point impacts on an accretion disk, typically generating a "hot spot." The motion of this stream was followed semi-analytically by Lubow and Shu (1975, 1976). The interaction between the stream and the accretion disk has been parameterized by Bath, Edwards, and Mantle (1983), in terms of a parameter β describing the rate of stripping of the stream material by the disk. Recently, this interaction has been studied both analytically and numerically by Livio, Soker, and Dgani (1986) and numerically by Rozyczka and Schwarzenberg-Czerny (1987, hereafter RS). Livio *et al.* (1986) attempted to obtain some aspects of the flow structure, treating the impact as a Sedov (1959) explosion. In addition, they presented a simplified three-dimensional numerical calculation of a steady state, in which the flow of the disk was assumed not to be affected by the stream. This calculation has demonstrated the fact that the stream flows above (and below) the disk surface. RS calculated the stream-disk interaction using a two-dimensional hydrodynamical code. They have shown that the hot region resulting from the collision covers $\sim \frac{1}{6}$ of the circumference of the disk and thus represents a "hot stripe" rather than a "hot spot."

In the present work, we extend the calculations of Livio *et al.* (1986), by relaxing some of the restricting assumptions made in the previous calculations. In particular, we include the effect of the stream impact on the disk material and we include the gravitational force of the accreting object. We are particularly interested in the time-dependent problem, obtained when the mass transfer rate in the stream is increased. Such a situation is expected in a dwarf nova eruption, if the mass transfer instability model is applicable (Bath 1975; Edwards 1987). The mass transfer rate also changes under other circumstances (e.g., TT Ari, Warner 1987).

The basic assumptions and method of calculation are described in § II, the results are presented in § III and discussed in § IV.

II. BASIC ASSUMPTIONS AND METHOD OF CALCULATION

We have used a pseudo-particle description of the three-dimensional hydrodynamics, as described by Livio *et al.* (1986). A polytropic equation of state was assumed for the unperturbed disk material and a steady state disk has been constructed assuming hydrostatic equilibrium in the z -direction (perpendicular to the plane of the disk). Unlike in the calculations of Livio *et al.* (1986), we followed the effects of the stream impact on the disk material (in a time-dependent way).

For the stream, we have used a Gaussian density profile, taken from Lubow and Shu (1975, 1976). Only a relatively small part of the disk, in the neighborhood of the point of impact has been calculated (see Fig. 1). This is due to memory limitations on a three-dimensional calculation.

We used for the parameters of the binary system: $M_1 = 1 M_\odot$, $q = M_2/M_1 = \frac{1}{7}$, a binary separation $a = 1.16 \times 10^{11}$ cm, $\dot{M} = 10^{16}$ g s $^{-1}$ (at quiescence). From these parameters we calculated the stream and disk quantities. The dimensions appearing in Figure 1 were taken as $XM = 9 \times 10^9$ cm, $YM = 1.5 \times 10^{10}$ cm, and $RH = 4 \times 10^{10}$ cm. In the numerical scheme, we used an average number of 10 particles per cell and performed calculations with the values of $\alpha = 1$ and $\alpha = 0.01$ for the strength of the interparticle interaction (see Livio *et al.* 1986 for details of the numerical method).

We would like to note that the mass ratio q was taken to be small, in order to minimize the gravitational effects from the secondary star, which were neglected in the calculation.

III. RESULTS

In the present work, we have been especially interested in the response of the stream-disk interaction region to an increase in the mass transfer rate. We therefore started the calculation from a steady state with $\dot{M} = 10^{16}$ g s $^{-1}$ and then increased \dot{M} linearly to $\dot{M} = 5 \times 10^{17}$ g s $^{-1}$ (over a period of 5000 s). We then continued the run until the establishment of a new steady state.

We performed three calculations, in which the polytropic exponent γ and the interparticle interaction strength α were taken as $\gamma = 1.2$, $\alpha = 0.01$ (run 1), $\gamma = 1.2$, $\alpha = 1$ (run 2) and $\gamma = 1.33$, $\alpha = 0.01$ (run 3). The general properties of the flows

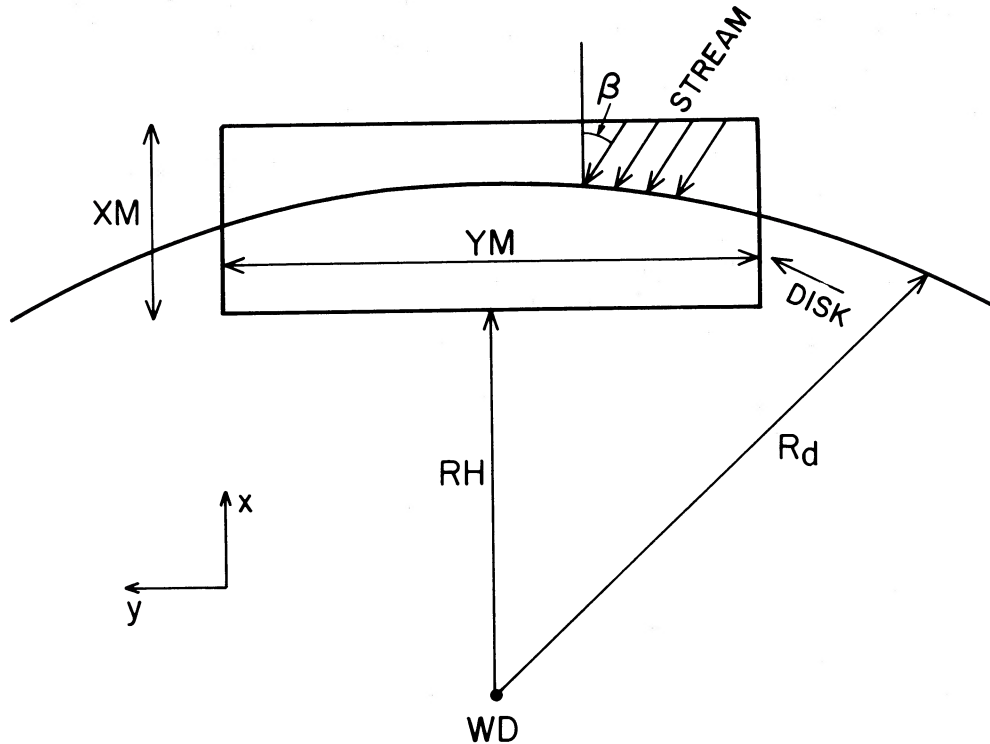


FIG. 1.—The location of the computational grid: $XM = 9 \times 10^9$ cm, $YM = 1.5 \times 10^{10}$ cm, $RH = 4 \times 10^{10}$ cm

obtained in runs 1 and 3 were similar. We observe the following features: (a) a low-mass reflected “jet,” (b) an expansion of the disk in the z -direction, and (c) a shock wave that forms in the disk (see Figs. 2–5). The total mass flux in the jet is low, resulting in a maximum of $\dot{M}_{\text{jet}} \approx 0.016\dot{M}_{\text{stream}}$ in run 3 (and only $0.0027\dot{M}_{\text{stream}}$ in run 1).

The angular momentum carried by the jet is not more than $\sim 10^{-3}$ of that in the impacting stream. Thus, we cannot expect this jet to remove all the angular momentum from the disk edge (and tidal interaction with the secondary is required). In both runs 1 and 3 the stream penetrates into the disk. This is a consequence of the relatively low value of α (which is proportional to the parameter β defining the rate of stream stripping, Bath *et al.* 1983). As the mass transfer rate is increased, two regions of enhanced density form above the plane of the disk (and below). This can be seen in Figure 6. One such region is the result of the stream flowing above the plane of the disk (Livio *et al.* 1986; Lubow and Shu 1976) and the second is caused by the expansion of the disk in the z -direction after passing through the interaction region (Fig. 7). The density above the disk reaches a value of $\sim 4 \times 10^{-10}$ g cm $^{-3}$ (starting from $\sim 7 \times 10^{-12}$ g cm $^{-3}$) in runs 1 and 3 and a value of $\sim 2 \times 10^{-9}$ g cm $^{-3}$ (starting from less than 10^{-12} g cm $^{-3}$) in run 2.

The shock formed within the disk (e.g., Fig. 4) is very similar to the shocks obtained by RS. However, due to the relatively poor resolution (imposed by memory constraints) of our three-dimensional calculation, we cannot resolve it into the two shocks obtained by these authors (the angle between the shocks is of order 6°).

The main differences between run 2 (in which the interparticle interaction is stronger) and runs 1 and 3 can be observed by examining Figures 8–12 (run 2) and comparing

them to Figures 2–5 (run 3). For the higher value of the stripping rate, the stream hardly penetrates into the disk (this is similar to RS). Instead, a region of high temperature and pressure (“hot stripe”) forms. In this case, a reflected stream also forms initially (Figs. 8–9), but at a much shallower angle than in runs 1 and 3.

The stream impacting on the disk has the effect of “pushing” the disk edge, as the mass transfer rate is increased. If we define as an “edge,” the location where the density in the disk has been reduced to less than 20% its initial value, then we obtain that this “edge” advances as shown in Figure 13 (for run 2). Due to the fact that our grid contains only a small fraction of the disk, we do not follow the changes in the disk radius globally. However, the deposition of relatively low specific angular momentum material from the stream results in a global shrinkage of the disk.

IV. DISCUSSION

We have presented time-dependent three-dimensional calculations of the stream-disk interaction region, relaxing many of the simplifying assumptions made in previous calculations. In particular, we have examined the response of the disk to an increase in the mass transfer rate.

In addition to the general interest in such two fluid interactions, some of the results of such (and similar) calculations can be used directly, in conjunction with observational data, to obtain valuable information on the accretion process and the system’s parameters. We shall now give a few examples.

a) Flow of the Stream above the Disk

We showed that (for certain system parameters) the stream of gas from L_1 can clear the edge of the disk, flow above (and

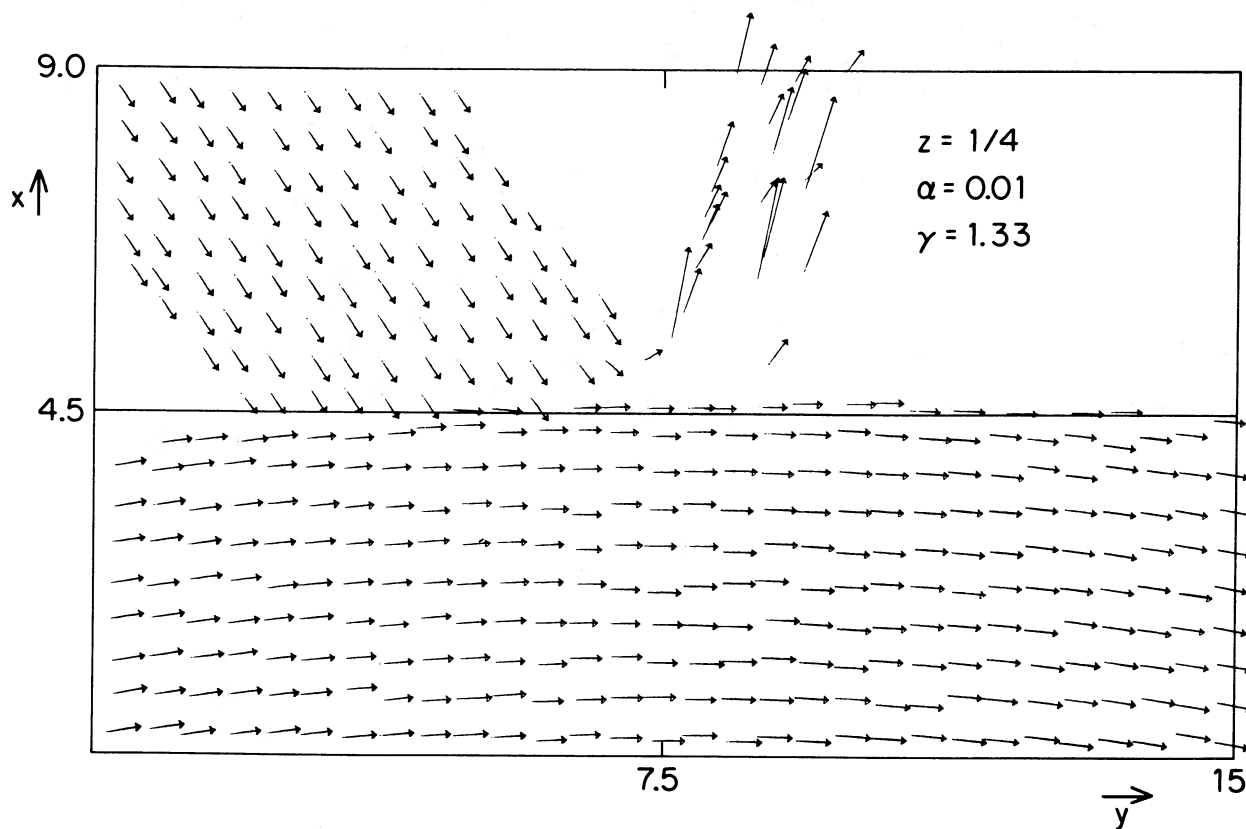


FIG. 2.—The flow pattern in the $z = 0.25z_0$ plane for run 3 (see text), at $t = 0$. The arrows are plotted at the center of mass of each grid cell. The length unit on the axes is z_0 (eq. [2]).

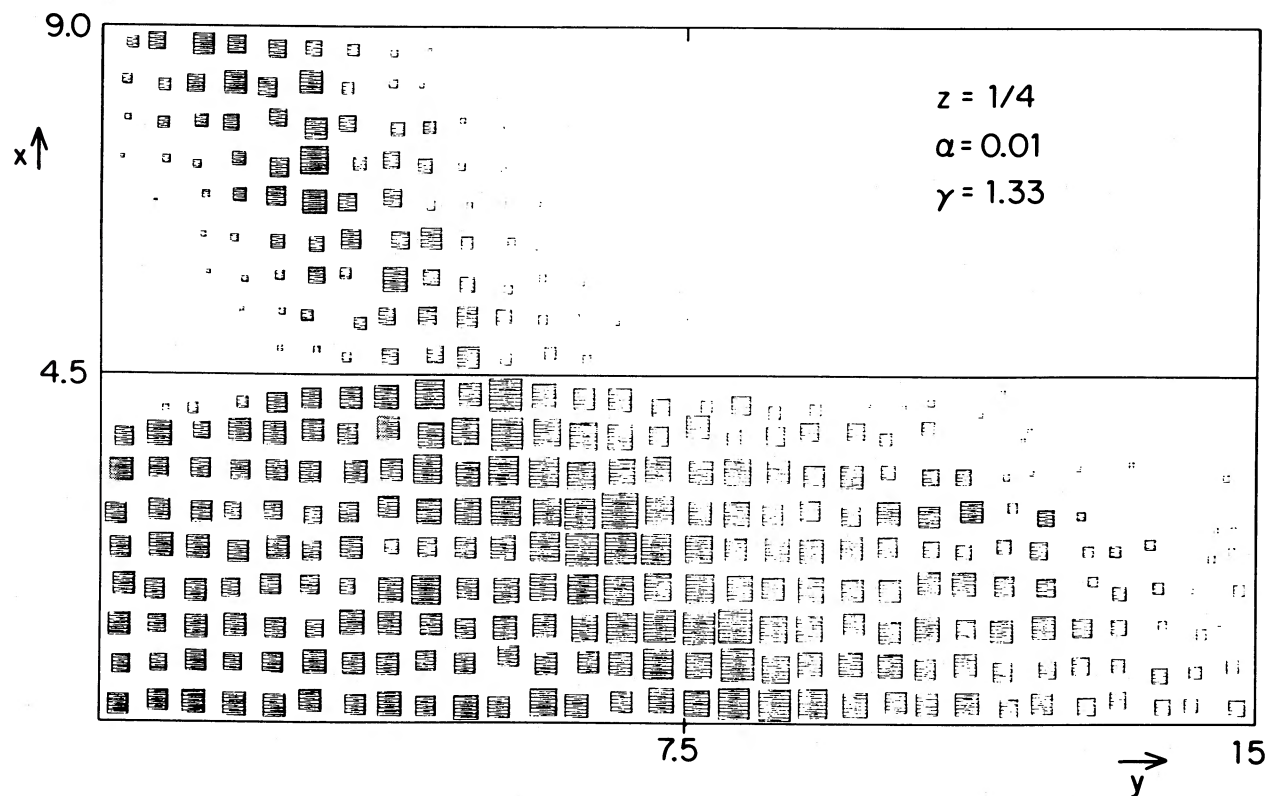


FIG. 3.—The density distribution corresponding to Fig. 4. The area of the squares is proportional to the density. The squares are plotted at the center of mass of each grid cell. The length unit on the axes is z_0 (eq. [2]).

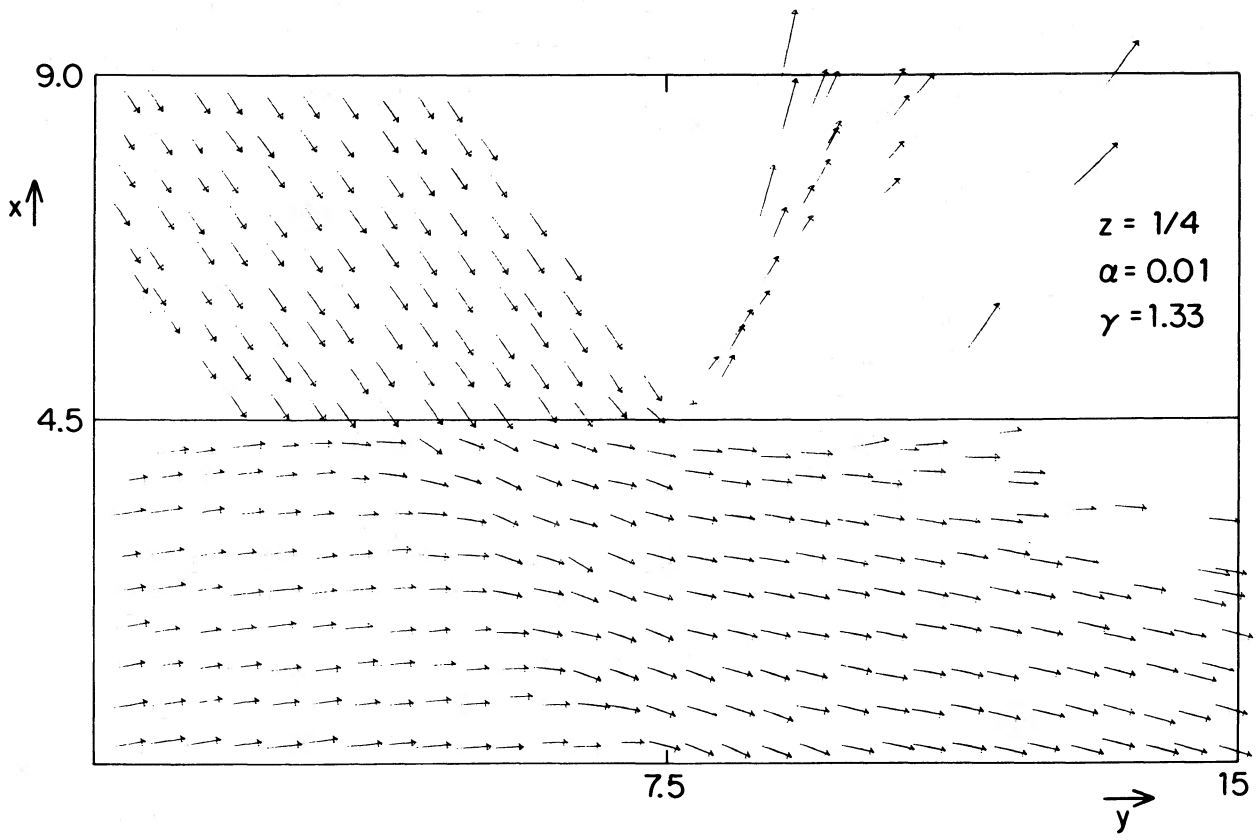


FIG. 4.—The flow pattern for run 3 (see text) at the end of the run (steady state)

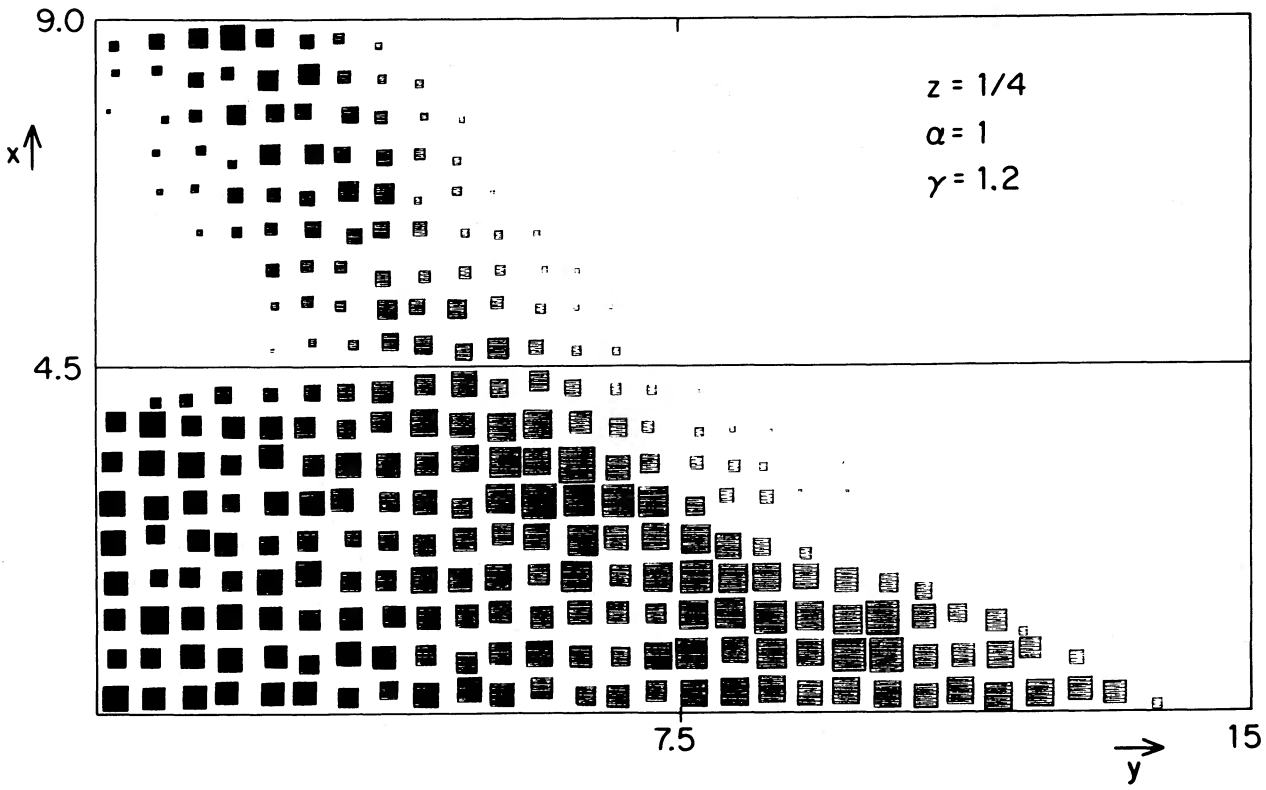


FIG. 5.—The density distribution in run 2 (see text) at $t = 4000$ s

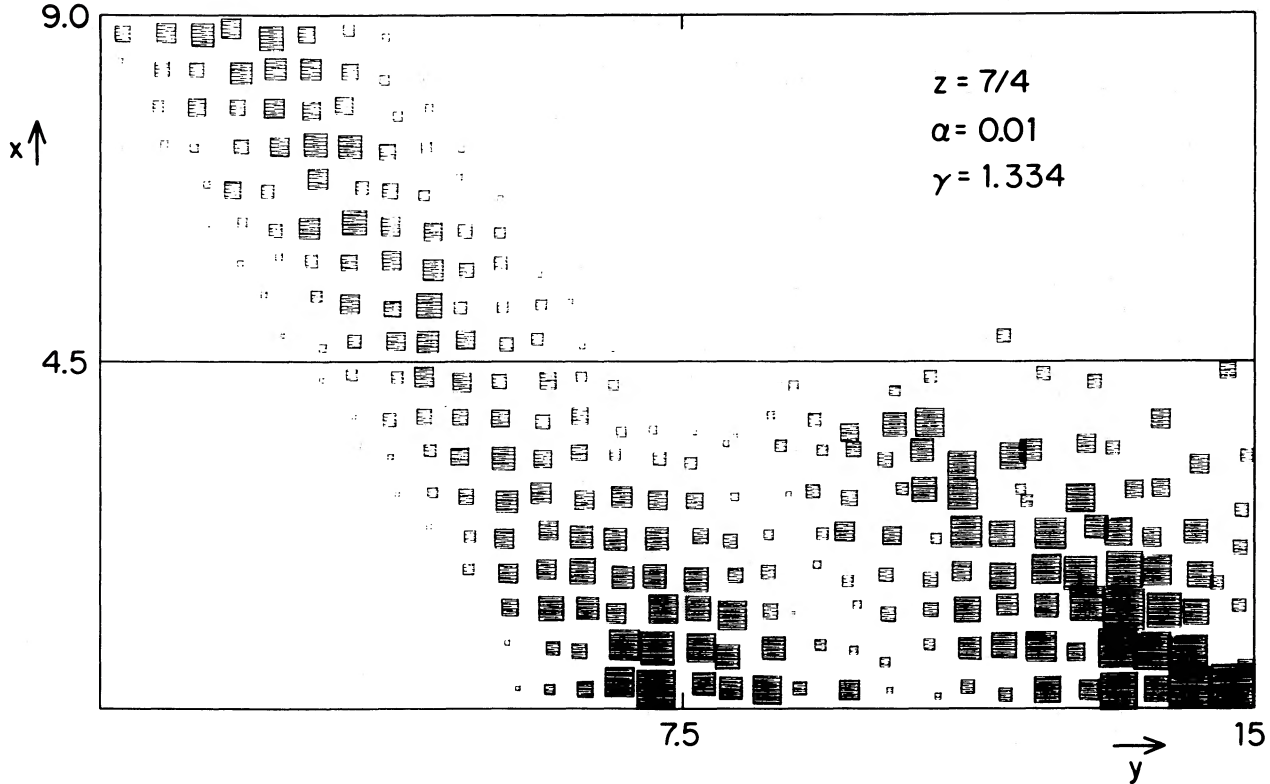


FIG. 6.—The density distribution in the plane $z = 1.75z_0$, at the end of the run for run 3

below) the disk and interact with disk material at a smaller radius. It is interesting to note that a Doppler tomogram of Z Cha (Marsh 1985) shows a curved emission feature along the continuation of the stream's trajectory inward from the hot spot, which could represent such a flow. We will now show that, in principle at least, an accurate determination of $\rho_s(z)/\rho_s$, where $\rho_s(z)$ is the density in the emission feature and ρ_s the central density of the stream, can give us the value of the Shakura-Sunyaev (1973) viscosity parameter α_{ss} . This is a con-

sequence of the fact that we find that the stream material penetrates above the disk when its density is comparable to that of the disk material $\rho_s(z) \sim \rho_d(z)$. Now, assuming a Shakura-Sunyaev disk and a stream structure from Lubow and Shu (1975, 1976) we obtain:

$$\frac{\rho_s(z)}{\rho_d(z)} = \frac{\rho_s}{\rho_d} \exp \left\{ - \left(\frac{z}{z_0} \right)^2 \left[\left(\frac{z_0}{H} \right)^2 - 1 \right] \right\}, \quad (1)$$

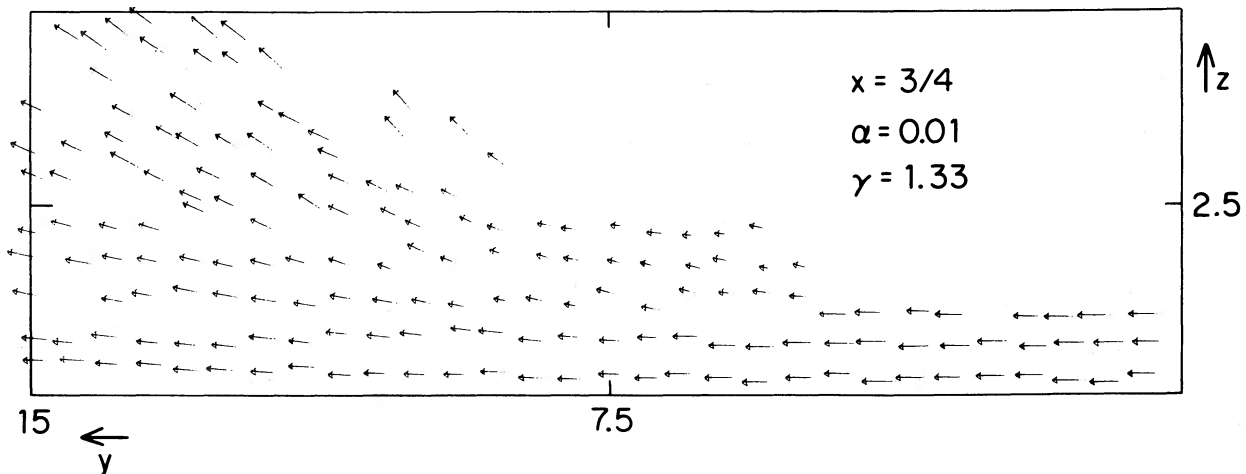
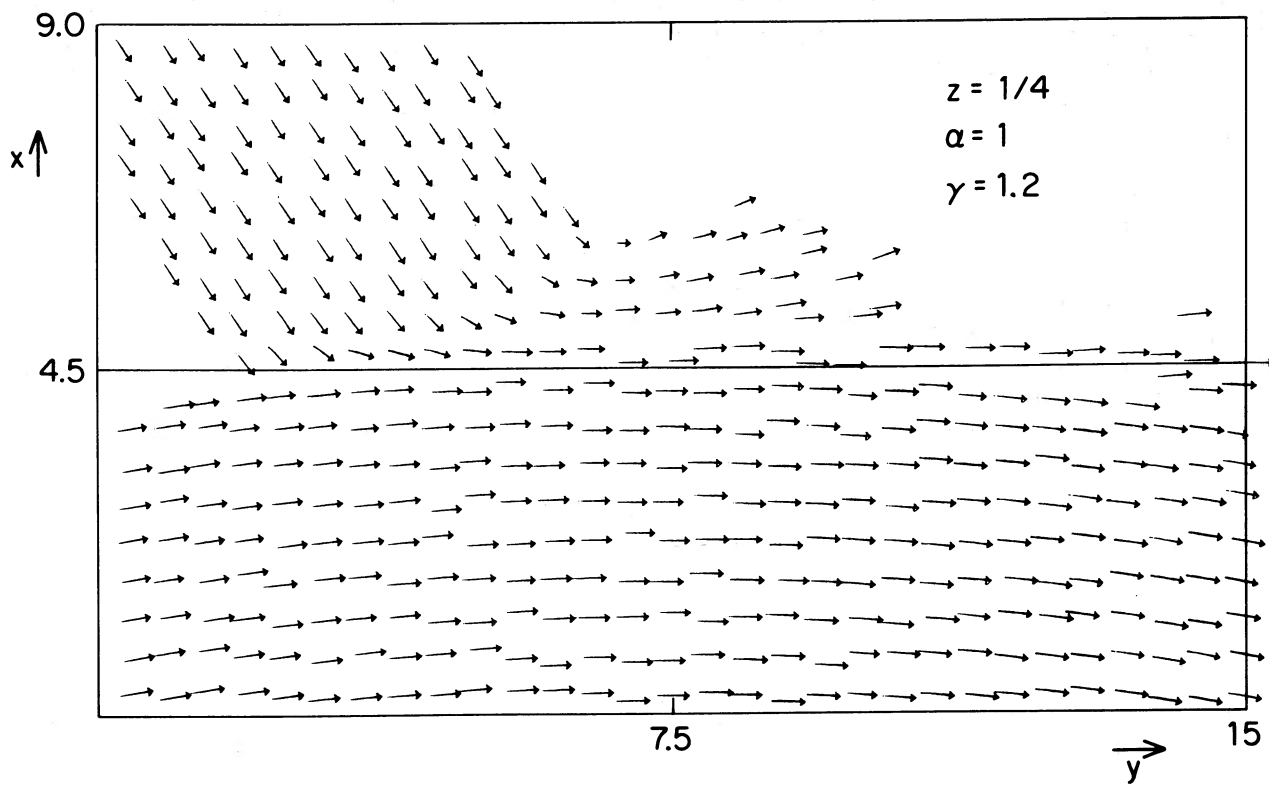
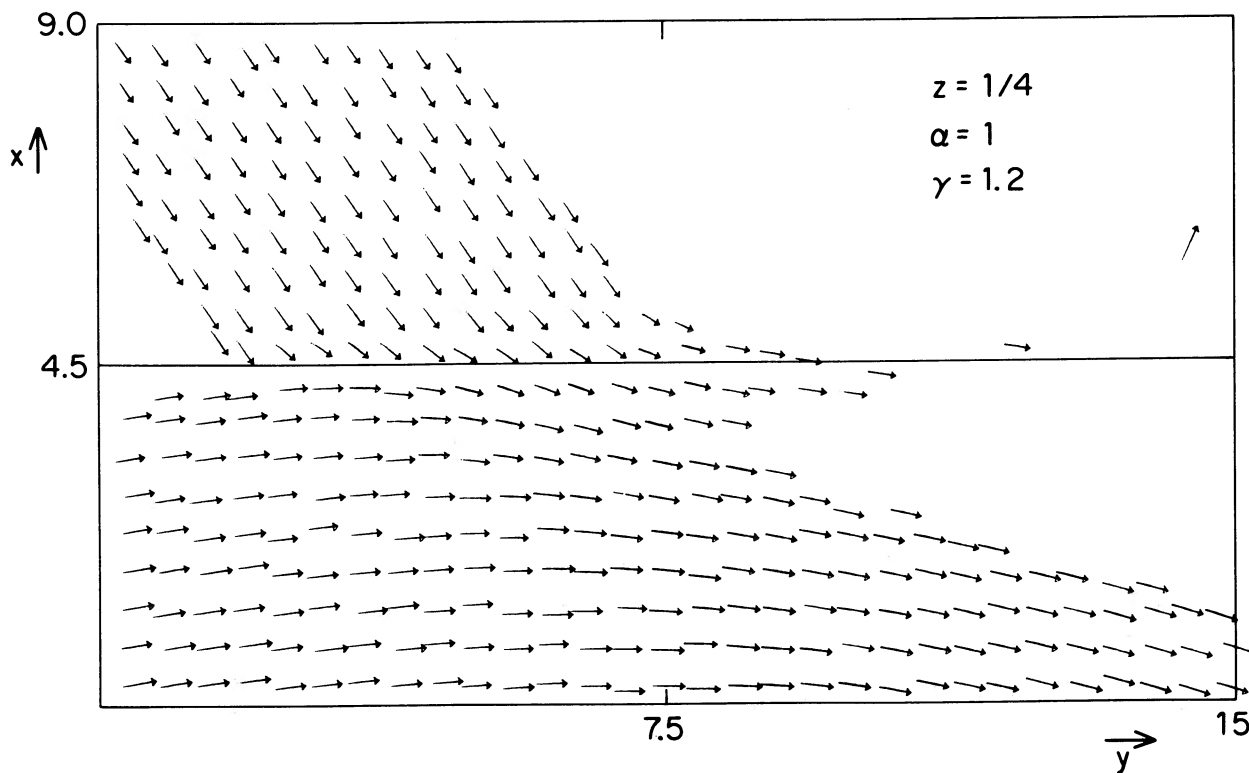


FIG. 7.—A side view of the expansion of the disk in run 3 (see text)

FIG. 8.—The flow pattern for run 2 (see text) at $t = 0$ FIG. 9.—The flow pattern for run 2 at $t = 2000$ s

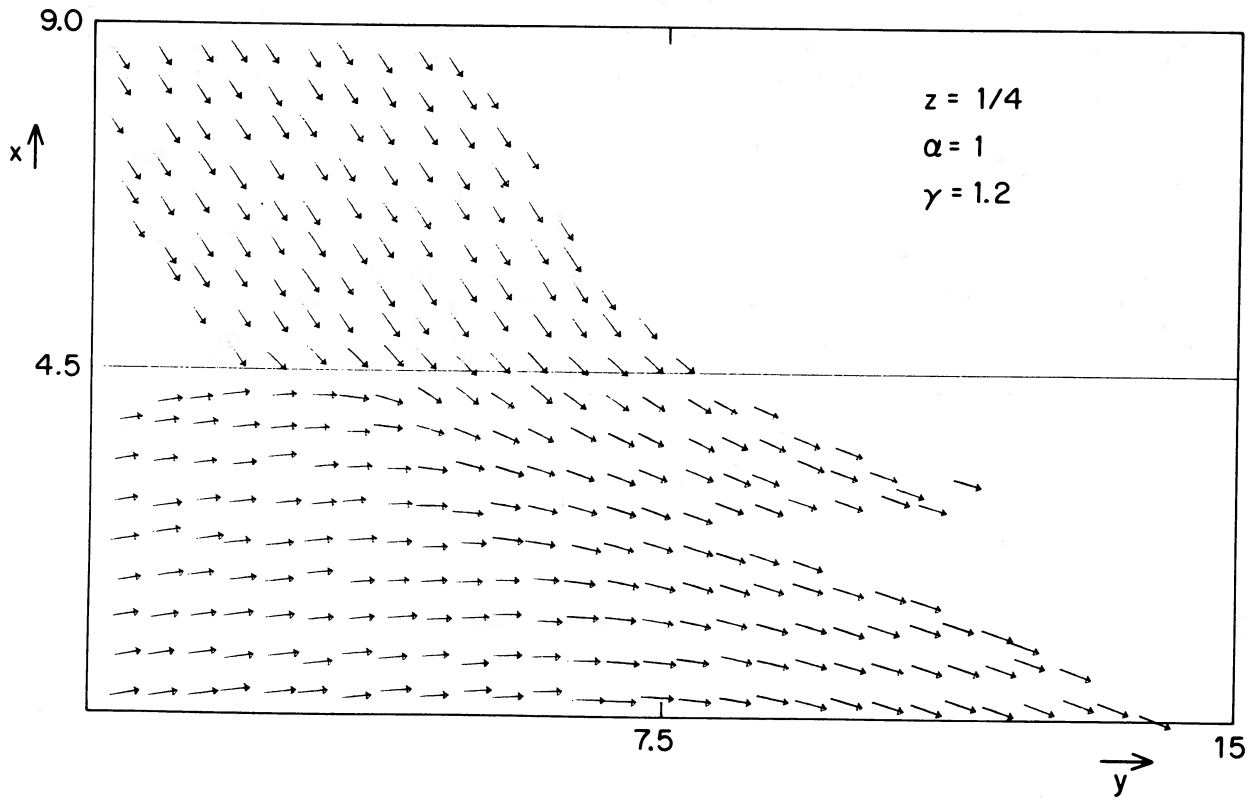
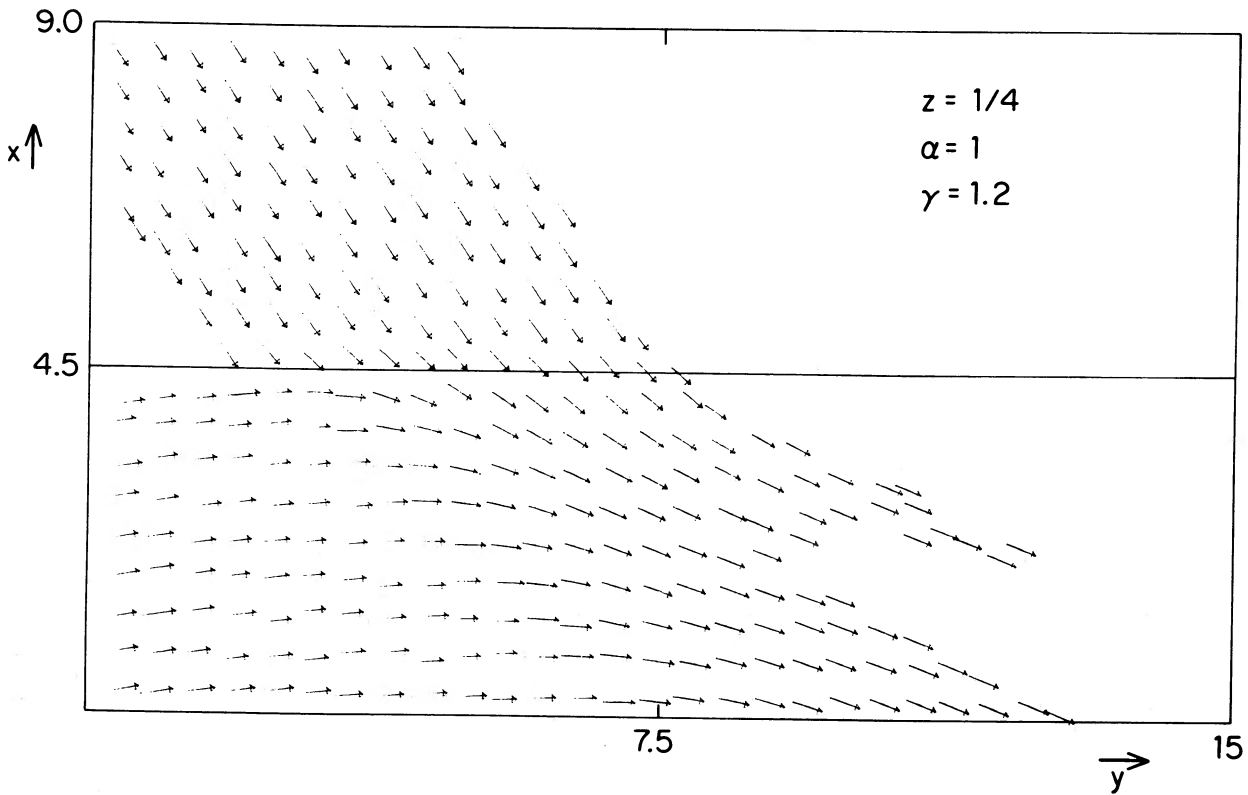
FIG. 10.—The flow pattern for run 2 at $t = 4000$ s

FIG. 11.—The flow pattern for run 2 at the end of the run (steady state)

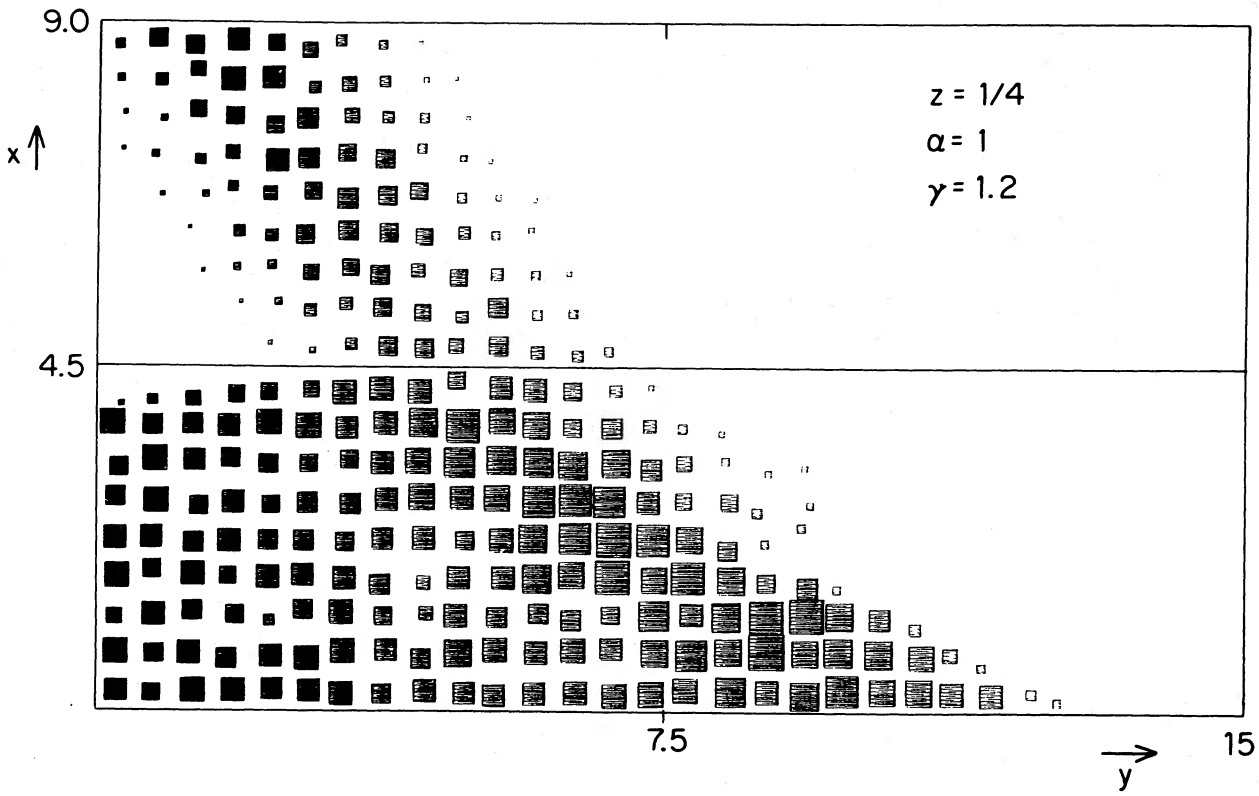


FIG. 12.—The density distribution for run 2 at the end of the run

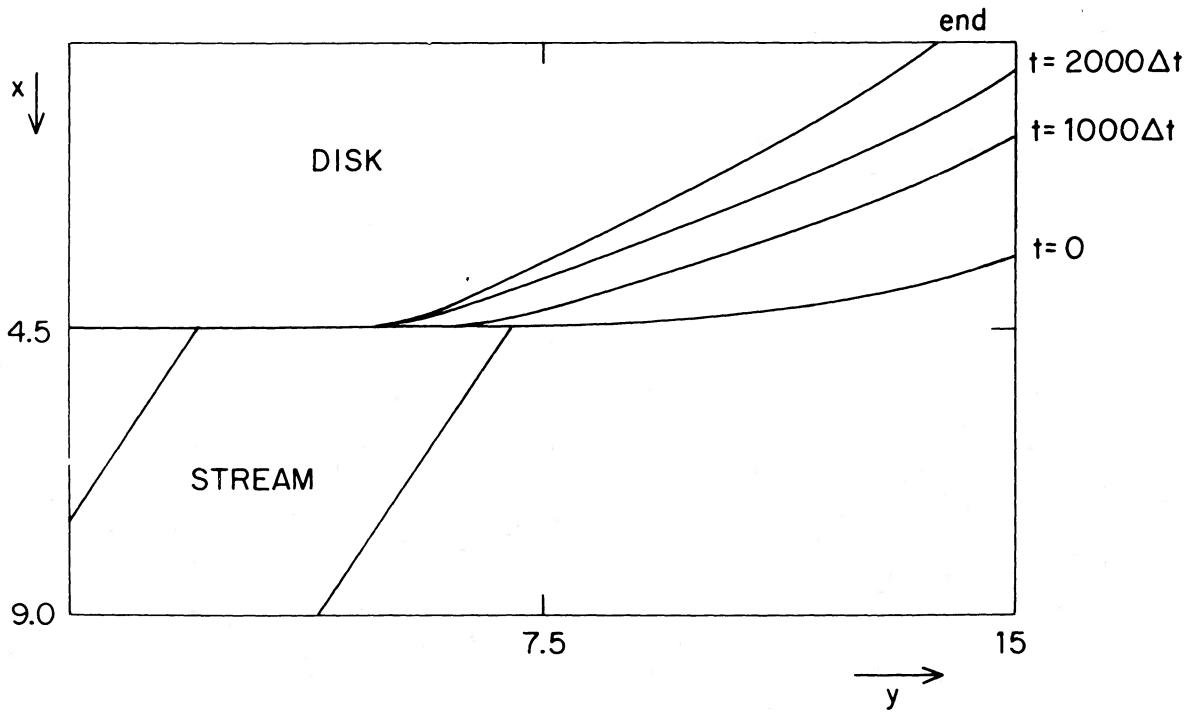


FIG. 13.—The location of the disk edge as a function of time for run 2 (see text). Here $\Delta t = 2$ s.

where

$$z_0 \approx 1.26 \times 10^8 \alpha_{\text{SS}}^{-1/10} \left(\frac{\dot{M}}{2.525 \times 10^{15} \text{ g s}^{-1}} \right)^{3/20} \times \left(\frac{M_{\text{WD}}}{0.65 M_{\odot}} \right)^{-3/8} \left(\frac{R_D}{1.41 \times 10^{10} \text{ cm}} \right)^{9/8} \text{ cm}, \quad (2)$$

$$\rho_d \approx 1.32 \times 10^{-8} \alpha_{\text{SS}}^{-7/10} \left(\frac{\dot{M}}{2.525 \times 10^{15} \text{ g s}^{-1}} \right)^{11/20} \times \left(\frac{M_{\text{WD}}}{0.65 M_{\odot}} \right)^{5/8} \left(\frac{R_D}{1.41 \times 10^{10} \text{ cm}} \right)^{-15/8} \text{ g cm}^{-3}, \quad (3)$$

$$\rho_s \approx 2.35 \times 10^{-10} \left(\frac{\epsilon}{0.01} \right)^{-2} \left(\frac{P_{\text{orb}}}{6.42 \times 10^3 \text{ s}} \right) \times \left(\frac{\dot{M}}{2.525 \times 10^{15} \text{ g s}^{-1}} \right) \times \left(\frac{a}{4.71 \times 10^{10} \text{ cm}} \right)^{-3} \text{ g cm}^{-3}, \quad (4)$$

$$H = 2.28 \times 10^8 \left(\frac{\epsilon}{0.01} \right) \left(\frac{a}{4.71 \times 10^{10} \text{ cm}} \right) \text{ cm}. \quad (5)$$

Here we have used parameters appropriate for Z Cha (Wood *et al.* 1986). The small parameter $\epsilon = (kT_{\text{eff}}/m)^{1/2}(\Omega a)^{-1}$ is of order 0.01 for Z Cha. From equations (1)–(5) we see that an observational determination of $\rho_s(z)/\rho_s$ can give us ρ_s/ρ_d , in which essentially all quantities are known from observations (except α_{SS}) and thus α_{SS} can be determined. Note in particular that ρ_s/ρ_d depends on the accretion rate only like $\dot{M}^{9/20}$, so that some uncertainty in the value of \dot{M} is not very important. Clearly, in practice, quite large uncertainties will be involved; however, it should be remembered that the value of α_{SS} at quiescence is not known even to within one order of magnitude! (For example, see Taam and McDermott 1987.)

b) Changes in the Disk Radius at Outburst

We have calculated the time dependent changes in the location of the disk edge in the neighborhood of the bright spot as the mass transfer rate is increased (Fig. 13). Previous global calculations (e.g., Bath *et al.* 1983) have also shown that the disk radius decreases initially during a mass transfer instability (unless very deep penetration occurs, at low values of β). This is a consequence of the deposition of low angular momentum material into the disk. However, following the initial decrease, the disk radius increases (Livio and Verbunt 1988).

On the other hand, in disk instability models (with the outburst starting at the outer edge), the disk radius is expected to increase at outburst. This is due to the increased viscosity, which causes most of the mass to move toward the accreting white dwarf, but the mass which takes the excess angular momentum spreads outward. Thus, a determination of the changes in the disk radius (in particular in the vicinity of the bright spot) at the outset of outbursts can provide us with a distinguishing criterion between the different dwarf nova eruption models (see also Verbunt 1986; Livio and Verbunt 1988).

In the case of U Gem, Smak (1984a) finds that an expansion of the disk begins near the onset of the outburst (in fact at $t = -2$). This has been shown to be consistent both with the disk instability models (e.g., Meyer and Meyer-Hofmeister 1984; Faulkner, Lin, and Papaloizou 1983; Cannizzo, Ghosh, and Wheeler 1982; Mineshige and Osaki 1983; Smak 1984b;

Duschl 1983), and with a mass transfer instability (Livio and Verbunt 1988). An interesting situation exists in the case of Z Cha. O'Donoghue (1986) finds that the disk radius is indeed higher following outburst and then shrinks, a behavior that is similar to that of U Gem. However, he also finds indications for a rather abrupt decrease in the radius a few days before the next outburst (followed by a sharp increase following the outburst). This has been shown to be consistent with a decrease caused by the impact of an increased mass transfer stream, followed by an increase associated with the higher mass transfer rate (Livio and Verbunt 1988). It should be noted, however, that due to the higher inclination of Z Cha ($i \approx 81^\circ.7$, Marsh, Horne, and Shipman 1987), the determination of the disk radius in this case is less certain (see also Anderson 1987).

The above discussion demonstrates that accurate monitoring of the disk radius prior to and during outbursts can potentially distinguish between the different dwarf nova outburst models.

c) The Angle of the Shock

This result has been discussed quite extensively by RS. In their high resolution two-dimensional calculation, the impacting stream generated two shocks inside the disk. In the present calculation, due to the relatively low resolution we could not resolve the two shocks. The shock that we obtained was found to form an angle of 40° to the direction of the flow of the unperturbed disk. In the case of Z Cha, it was found that the plane of the shock lies approximately half way between the stream velocity and the Keplerian velocity vectors (K. Horne 1987, private communication). For relatively large values of the stream impacting angle β (Fig. 1) the angle between the shock and the direction of the flow in the disk is $\delta \sim (90 - \beta)/3$ (see RS). Again, therefore, an accurate determination of the shock(s) angle(s), can in principle provide information on some of the system parameters.

d) Hot Spot Luminosity

In the mass transfer instability, the luminosity of the hot spot is expected naively to increase at outburst, due to the increased mass transfer rate. In the disk instability model the hot spot luminosity can be expected to decrease somewhat, due to the expansion of the disk, which makes the potential well more shallow.

Past observations have claimed a very moderate increase in the hot spot luminosity if any (e.g., Vogt 1983; Haefner, Schoembs, and Vogt 1979). It should be remembered, however, that the observed orbital hump measures only the flux which can produce an asymmetric radiation pattern. In the present calculation, we estimated the relative increase in the luminosity, generated near the impact region, by calculating the energy dissipated as a function of time. We find that the maximum relative increase in the dissipation rate was by a factor ~ 8 (while \dot{M} was increased by a factor of 50). This moderate increase is mostly due to stream penetration. Thus, stream penetration can indeed result in an increase in the hot spot's luminosity, which is much more moderate than that expected if all the kinetic energy would have been dissipated at the outer edge. More calculations will be required, to establish where and how the hot spot flux is emitted.

To conclude—the results of the present and similar calculations can be used, together with observations, to both determine parameters of the systems involved and to distinguish between theoretical models.

We are grateful to M. Rozyczka and A. Schwarzenberg-Czerny for showing us their results prior to publication.

This research has been supported in part by NSF grant AST86-11500 at the University of Illinois and by NASA Astro-

physical Theory Center grant NAGW-764 at the University of Virginia. M. L. wishes to thank the Max-Planck-Institut für Astrophysik, where a part of this work has been completed, for its generous hospitality.

REFERENCES

- Anderson, N. 1987, preprint.
 Bath, G. T. 1975, *M.N.R.A.S.*, **171**, 311.
 Bath, G. T., Edwards, A. C., and Mantle, V. J. 1983, in *IAU Colloquium 72, Cataclysmic Variables and Related Objects*, ed. M. Livio and G. Shaviv (Dordrecht: Reidel), p. 55.
 Cannizzo, J. K., Ghosh, P., and Wheeler, J. J. C. 1982, *Ap. J. (Letters)*, **260**, L83.
 Duschl, W. J. 1982, *Astr. Ap.*, **121**, 153.
 Edwards, D. 1984, *M.N.R.A.S.*, **226**, 95.
 Faulkner, J., Lin, D. N. C., and Papaloizou, J. 1983, *M.N.R.A.S.*, **205**, 359.
 Haefner, R., Schoembs, R., and Vogt, N. 1979, *Astr. Ap.*, **77**, 7.
 Livio, M., Soker, N., and Dgani, R. 1986, *Ap. J.*, **305**, 267.
 Livio, M., and Verbunt, F. 1988, *M.N.R.A.S.*, **232**, 1 p.
 Lubow, S. H., and Shu, F. H. 1975, *Ap. J.*, **198**, 383.
 ———. 1976, *Ap. J. (Letters)*, **207**, L53.
 Marsh, T. R. 1985, Ph.D. thesis, Cambridge University, England.
 Marsh, T. R., Horne, K., and Shipman, H. L. 1987, preprint.
 Meyer, F., and Meyer-Hofmeister, E. 1984, *Astr. Ap.*, **132**, 143.
 Mineshige, S., and Osaki, Y. 1983, *Pub. Astr. Soc. Japan*, **35**, 377.
 O'Donoghue, D. 1986, *M.N.R.A.S.*, **220**, 23 p.
 Rozyczka, M., and Schwarzenberg-Czerny, A. 1987, *Acta Astr.*, **3R**, 141 (RS).
 Sedov, L. I. 1959, *Similarity and Dimensional Methods in Mechanics* (London: Infosearch, Ltd.).
 Shakura, N. I., and Sunyaev, R. A. 1973, *Astr. Ap.*, **24**, 33.
 Smak, J. 1984a, *Acta Astr.*, **34**, 93.
 ———. 1984b, *Acta Astr.*, **34**, 161.
 Taam, R. E., and McDermott, P. N. 1987, *Ap. J. (Letters)*, **319**, L83.
 Verbunt, F. 1986, in *Physics of Accretion onto Compact Objects*, ed. K. O. Mason, M. G. Watson, and N. E. White (Berlin: Springer Verlag), p. 59.
 Vogt, N. 1983, *Astr. Ap.*, **128**, 29.
 Warner, B. 1987, *M.N.R.A.S.*, **227**, 23.
 Wood, J., Horne, C., Berriman, G., Wade, R. A., O'Donoghue, D., and Warner, B. 1986, *M.N.R.A.S.*, **219**, 629.

RUTH DGANI: Department of Mathematics, Technion, Haifa 32000, Israel

MARIO LIVIO: Department of Physics, Technion, Haifa 32000, Israel

NOAM SOKER: Department of Astronomy, University of Virginia, Charlottesville, VA 22903